Comparative study of *ab initio* and tight-binding electronic structure calculations applied to platinum surfaces

S. Baud* and C. Ramseyer

Laboratoire de Physique Moléculaire, UMR CNRS 6624, Université de Franche-Comté, F-25030 Besançon Cedex, France

G. Bihlmayer and S. Blügel

Festkörperforschung, Forschungzentrum Jülich, 52425 Jülich, Germany

C. Barreteau and M. C. Desjonquères

DSM/DRECAM/SPCSI, CEA Saclay, Bâtiment 462, F-91 191 Gif sur Yvette, France

D. Spanjaard

Laboratoire de Physique des Solides, Université Paris Sud, F-91 405 Orsay, France

N. Bernstein

Center for Computational Materials Science, Naval Research Laboratory, Washington, D.C., 20375, USA

We have applied the full-potential linearized augmented plane-wave (FLAPW) *ab initio* method and the *spd* tight-binding (TB) model to the calculations of the surface energies $E_S(hkl)$ and relaxations of the three low-index [(111), (100), (110)] surfaces of platinum. The two methods give similar results, and in particular the anisotropy ratios $E_S(110)/E_S(111)$ and $E_S(100)/E_S(111)$ are very close. The calculation of surface energy of reconstructed (1×2) Pt(110) confirms that this face undergoes a missing-row reconstruction and the corresponding structural parameters agree well with experiment. The local densities of states (LDOS) calculated by each of the methods on the flat surfaces are almost the same. We have also investigated the $6(111) \times (\bar{1}11)$ vicinal surface and found a similar agreement for the LDOS.

PACS number(s): 68.35.Md, 71.15.Ap, 71.15.Mb, 71.20.−b

I. INTRODUCTION

The surface energy represents a fundamental property of materials. It is defined as the energy (per surface atom or per unit surface area) needed to split an infinite crystal into two semi-infinite crystals bounded by a crystallographic plane with a given orientation. A variety of experimental techniques has been developed to measure the surface energy,[1] but all measurements are performed at high temperatures where surfaces are badly defined. Most experimental data[2,3] stems from surface tension measurements in the liquid phase and by extrapolating the orientation-averaged surface free energies to zero temperature. However, a detailed knowledge of surface properties is necessary to predict the equilibrium shape of a mesoscopic crystal and is important for the understanding of a wide variety of phenomena such as catalysis, surface reactivity, growth, creation of steps and kinks on surfaces, etc.

The lack of experimental data can be replaced by calculations of different kinds. Generally, two main types of calculations are used, based either on semi-empirical potentials [embedded atom model (EAM),[4] second moment approximation (SMA),[5] effective medium theory (EMT),[6] Sutton-Chen and Finnis-Sinclair potentials[7]] or on the determination of the electronic structure from density functional theory (DFT) or parametrized Hamiltonians such as tight-binding (TB) models. The first calculations of the surface energy of transition metals were performed using the TB scheme based on

a pure *d* band model.[8–10] These first results gave an interpretation of the roughly parabolic variation of surface energies along the transition-metal series since, for these elements, the cohesive properties of the solid are governed by the *d* electrons. Quantitative results were found for elements that are not too close to the beginning or the end of the series. On the contrary, when the *d* band is almost filled or empty, the *sp* band plays a non-negligible role in the cohesive properties and thus the results obtained with a pure *d* band were, at best, qualitative.[10] In order to improve the model, *spd* tight-binding methods were developed.[11]

Due to the development of the DFT during the last two decades, *ab initio* methods can now be used to calculate many physical properties with unprecedented accuracy. Methfessel *et al.*[12] have done a pioneering work in determining the surface energy, work function, and relaxation for the whole series of bcc and fcc 4*d* transition metals, using a full-potential version of the linear muffin-tin orbital (FP-LMTO) method in conjunction with the local density approximation (LDA) to the exchange-correlation potential. In the same spirit, Skriver and co-workers[13,14] have used a LMTO technique to determine the surface energy and the work function of most of the elemental metals. For Pt, a first attempt has been done by Feibelman using LDA in a basis of contracted Gaussian orbitals.[15] Vitos *et al.*,[16] using full-charge Green's function LMTO technique in the atomic sphere approximation (ASA) in conjunction with the generalized gradient approximation (GGA), have elaborated a

very useful database that contains the low-index surface energies for 60 metals of the periodic table, but neglecting atomic surface relaxation. In the last decades, several full-potential linearized augmented plane-wave (FLAPW) calculations have also been carried out for the 3*d* and 4*d* transition metals.[16] In contrast, the 5*d* series has been much less studied with this method except for tungsten surfaces.[17,18]

The two methods, *ab initio* or TB, have their own advantages and drawbacks. The strength of *ab initio* calculations is their high transferability and predictive power, but they remain, compared with TB methods, lengthy and are usually restricted to systems with a limited number of inequivalent atoms. TB calculations mostly rely on some parameters whose transferability has sometimes been questioned but which can produce quantitative results for systems with a large number (up to a few thousands) of geometrically inequivalent atoms. Thus TB methods open up the possibility of studying rough surfaces, homoepitaxial growth, step flow growth, surface melting, or cluster deposition. Indeed such problems would be difficult to model with *ab initio* methods due to the CPU time required even on very powerful computers. In any case before using a set of TB parameters in such systems, it is necessary to first check that this set produces results in good agreement with *ab initio* calculations on simple systems.

In this work, we have mainly investigated the low-index surface energies of platinum. Indeed, the study of low-index surfaces is a prerequisite to that of vicinal surfaces of platinum which are often used as a template to construct self-organized structures such as nanowires[19,20] displaying specific magnetic or electronic properties. Moreover, strong couplings between these nanostructures and the substrate could occur. A detailed knowledge of the electronic properties of such surfaces is thus needed for future work. Here, we focus on the main crystallographic faces of platinum [(111), (100), and (110)]. In particular, we have calculated the surface energies $E_S(hkl)$ and compared the results given by an *ab initio* method based on a full-potential scheme to a *spd* TB model. In addition, we have also investigated the missing-row reconstruction of the (110) surface and the $6(111) \times (\bar{1}11)$ vicinal surface.[21] This paper is organized as follows. In Sec. II, we summarize briefly the two methods. In Sec. III the results are presented and discussed. Concluding remarks are given in Sec. IV.

II. COMPUTATIONAL METHODS

A. The FLAPW method

The results were obtained with the FLAPW in bulk and film geometry[22] as implemented in the computer code FLEUR,[23] based on density functional theory in LDA or GGA. For LDA we used the exchange-correlation (XC) potential of von Barth and Hedin,[24] and for GGA the version of Perdew *et al.*[25] The surfaces were modeled by slabs with n ($n \geqslant 11$) atomic layers of Miller indices (hkl). The Pt muffin-tin radius was set equal to 2.3 a.u. (1.219 Å). Inside each muffin-tin sphere, the charge density and the potential were expanded in spherical harmonics with angular momentum up to

$l=8$. Throughout this paper, the total-energy results have been obtained using basis functions including wave vectors up to $k_{max}=4$ a.u. amounting to around 130 basis functions per atom. Within the irreducible wedge of the two-dimensional Brillouin zone (BZ), eigenvalues and eigenvectors were calculated using different sets of Monkhorst-Pack[26] **k** or $\mathbf{k}_\parallel$ points. The calculations of bulk Pt were performed with 216 **k** points in the irreducible wedge of the three-dimensional BZ. In order to keep an equivalently dense mesh in the two-dimensional BZ (2DBZ) we used a special $\mathbf{k}_\parallel$-point set of 57 points within 1/6 of the 2DBZ for the (111) face, 48 $\mathbf{k}_\parallel$ points within 1/4 of the 2DBZ for the (110) face and 36 $\mathbf{k}_\parallel$ points within 1/8 of the 2DBZ for the (100) face. Self-consistency was achieved when the root-mean-square difference between the input and the output charge densities was less than 2×10^{-4} electrons/(a.u.)^3, which has been proved to be sufficient.

B. The *spd* tight-binding method

Let us briefly describe the *spd* TB model for platinum. A nonorthogonal minimal basis set of *s*, *p*, and *d* valence atomic orbitals $|i\lambda\rangle$ is assumed, $|i\lambda\rangle$ denoting the orbital λ centered at site i. Indeed platinum is at the end of the 5*d* series and *s* and *p* electrons, which are better described in a nonorthogonal scheme, play a significant role in cohesive properties. In this basis, solving the Schrödinger equation requires the knowledge of the matrix elements (on-site and intersite) of the Hamiltonian and of the overlap matrix. The intersite matrix elements of the Hamiltonian are limited to two-center integrals. All these matrix elements are assumed to obey given functional forms as a function of the inter-atomic distance including parameters that are determined using a nonlinear least mean square fit on *ab initio* bulk band structure and total-energy curve for typically 4–6 interatomic distances and two crystallographic structures, bcc and fcc. The corresponding functional forms and parameters can be found in Ref. 11. One should note that these parameters are obtained from systems in which all atoms are neutral since they are geometrically equivalent. When this is not the case, for instance, in the presence of a surface, a shift δV_i is added to the on-site terms in order to account for the effect of the charge redistribution occurring at the surface. However, the nonorthogonality leads to a generalized eigenvalue problem. In this case it is well known that a rigid shift of the on-site matrix elements of the Hamiltonian does not produce a rigid shift of the eigenvalues.[27] The potential that must be added to the Hamiltonian matrix $H_{ij}^{\lambda\mu}$ to produce a rigid shift δV_0 of the eigenvalues has the following expression in the atomic orbital basis:[27]

$$\delta V_{ij}^{\lambda\mu} = \langle i\lambda | \delta V | j\mu \rangle = \delta V_0 S_{ij}^{\lambda\mu}, \quad (1)$$

where $S_{ij}^{\lambda\mu}$ is the overlap integral between orbital $|i\lambda\rangle$ and orbital $|j\mu\rangle$. The generalization of this formula to the case of an inhomogeneous system is straightforward:

$$\delta V_{ij}^{\lambda\mu} = \langle i\lambda | \delta V | j\mu \rangle = \frac{1}{2}(\delta V_i + \delta V_j)S_{ij}^{\lambda\mu}. \qquad (2)$$

Of course one has to subtract the double counting term due to electron-electron interactions, which has exactly the same expression as in the orthogonal case, i.e.,

$$E_{dc} = N_{val}\sum_i \delta V_i + \frac{1}{2}\sum_i \delta V_i \delta N_i, \qquad (3)$$

where N_{val}, N_i, and δN_i are, respectively, the total number of valence electrons per atom of the metal, the Mulliken population of atom i, and its Mulliken net charge. As in Ref. 28 the following relation,

$$\delta V_i = U \delta N_i, \qquad (4)$$

has been assumed with $U=5$ eV. The local charges δN_i are determined self-consistently and obey $\Sigma_i \delta N_i = 0$. Consequently the double counting term in the total energy reduces to

$$E_{dc} = \frac{1}{2}\sum_i U_i(\delta N_i)^2. \qquad (5)$$

The summations over the 2DBZ, involved in the TB calculations, were performed using 135, 136, and 256 Cunningham special $\mathbf{k}_\parallel$ points[29] in the irreducible wedges of the (111), (100), and (110) 2DBZ, respectively.

III. RESULTS

In this section, we present all the results we have obtained using the full-potential method and the *spd* TB method. The bulk structural features calculated with the two methods agree well with the available experimental data. With the computer code FLEUR, we have determined the theoretical Pt bulk lattice constant, a_0, and bulk modulus, B_0, to be equal to 3.89 Å and 3.14 Mbar, respectively, within the LDA approximation, and to 3.98 Å and 2.59 Mbar, respectively, within the GGA approximation. These values are in good agreement with the experimental values of 3.92 Å and 2.78 Mbar,[30] respectively. Nevertheless, as mentioned in other works,[31–34] we find that LDA offers better agreement for the lattice constant (−0.43% compared to experiment) than GGA (+1.71% compared to experiment). In addition the bulk modulus is overestimated (underestimated) with LDA (GGA). This is clearly connected to the underestimation (overestimation) of the lattice parameters obtained with LDA (GGA). Within the *spd* TB theory, the calculated lattice parameter is 3.90 Å. This value only differs by 0.25% from the experimental one. The bulk modulus (3.06 Mbar) is close to the value obtained with LDA. This was rather expected since the TB parameters have been fitted to LDA calculations.[11] The calculated lattice parameters will be used in the following.

A. Electronic structure of the low-index surfaces

We start this study by considering unrelaxed surfaces, and first we compare the band structures obtained for the (111)
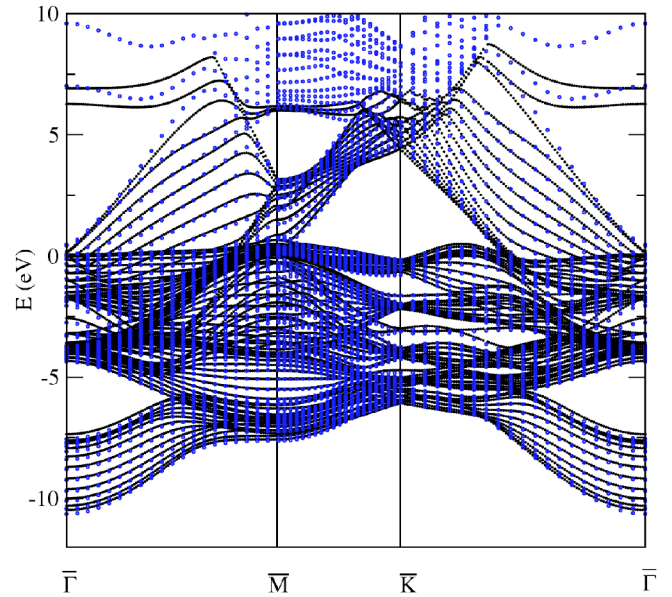

FIG. 1. (Color online) The surface band structure of Pt(111). Dotted lines (black) correspond to the FLAPW method and circles (blue) to *spd* TB calculations. Both FLAPW and TB calculations were done using a 13 layers slab. The zero energy is taken at the Fermi level.

face of platinum using *ab initio* and TB methods. The agreement is almost perfect, up to 5 eV above the top of the *d* band, for the projected bulk band structure as well as for the
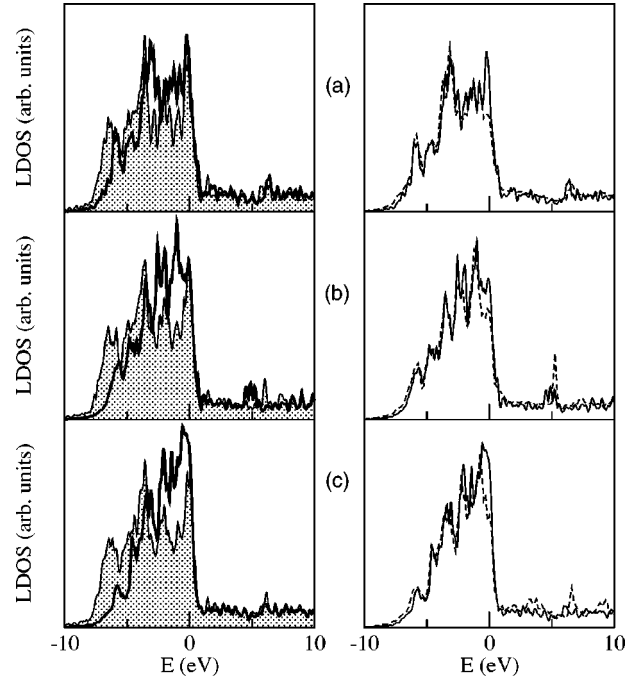

FIG. 2. Left column: LDOS on the bulklike atoms, i.e., belonging to the central layer of the slab (shaded parts) and the surface atoms (solid lines) in the case of FLAPW calculations. Right column: LDOS on the surface atoms obtained with the FLAPW method (solid lines), and *spd* TB calculations (dashed lines). (a) (111), (b) (100), and (c) (110). The origin of the energy scale refers to the Fermi energy.

TABLE I. Electronic valence charge of *s*, *p*, and *d* character in the muffin-tin sphere (FLAPW) or projected on the atomic orbitals (*spd* TB) of the different (*hkl*) films for unrelaxed geometries. The surface, first subsurface, and central atomic layers are denoted as S, S−1, and C, respectively.

Orientation	Atom	FLAPW				TB			
		s	*p*	*d*	Total	*s*	*p*	*d*	Total
(111)	Pt(C)	0.379	0.282	7.136	7.845	0.696	0.679	8.605	9.978
	Pt(S−1)	0.374	0.277	7.135	7.835	0.694	0.664	8.629	9.987
	Pt(S)	0.385	0.218	7.133	7.770	0.795	0.622	8.684	10.101
(100)	Pt(C)	0.379	0.281	7.135	7.844	0.696	0.678	8.600	9.975
	Pt(S−1)	0.376	0.277	7.125	7.827	0.701	0.675	8.602	9.978
	Pt(S)	0.376	0.189	7.162	7.758	0.797	0.560	8.776	10.136
(110)	Pt(C)	0.379	0.282	7.133	7.843	0.696	0.677	8.602	9.975
	Pt(S−1)	0.377	0.263	7.109	7.794	0.727	0.689	8.592	10.008
	Pt(S)	0.365	0.164	7.198	7.752	0.784	0.503	8.869	10.156

dispersion curves of the surface states present in the gaps (Fig. 1). Another interesting quantity describing the surface electronic structure is the local density of states (LDOS) on atoms belonging to successive layers. In both methods they are defined starting from the LDOS $n(\mathbf{r},E)$ at point $\mathbf{r}$:

$$n(\mathbf{r},E) = \sum_n |\psi_n(\mathbf{r})|^2 \delta(E - E_n), \qquad (6)$$

where $\psi_n(\mathbf{r})$ and E_n are the eigenfunctions and the eigenvalues, respectively. In the FLAPW method the LDOS at site i is defined as the integral of $n(\mathbf{r},E)$ over the muffin-tin sphere S_i centered at site i, i.e.,

$$n_i(E) = \sum_n \delta(E - E_n) \int_{S_i} |\psi_n(\mathbf{r})|^2 d^3\mathbf{r}. \qquad (7)$$

In the TB approach, $\psi_n(\mathbf{r})$ is written as a linear combination of atomic orbitals $|i\lambda\rangle$ with coefficients $c_{i\lambda}(E_n)$. The total density of states is obtained by integrating Eq. (6) over the whole space. This can be written

$$n(E) = \sum_i n_i(E), \qquad (8)$$

thereby defining the LDOS $n_i(E)$ as

$$n_i(E) = \sum_{n,j,\lambda,\mu} c_{i\lambda}^*(E_n) c_{j\mu}(E_n) S_{ij}^{\lambda\mu} \delta(E - E_n). \qquad (9)$$

Thus the LDOS calculated with the two methods are not expected to be strictly the same.

In Fig. 2, we present the LDOS $n_i(E)$ for two different sites i of the three different faces using the two methods (note that they have been renormalized). The shapes of these LDOS are very similar. In both methods we observe the well-known overall narrowing of the LDOS on surface atoms. However, the amplitudes of the LDOS are slightly different especially at the Fermi level. Indeed, in any case the LDOS are dominated by the *d* electron contribution and should be very similar when these electrons are almost completely contained inside the S_i sphere. In the present case

around 80% of the *d* electrons are inside S_i (see Table I). This is the reason for the similarity of the LDOS obtained with the two methods. However, the *d* wave functions near the Fermi level have an antibonding character and thus extend less outside S_i. This qualitatively explains the differences found near the Fermi level. This argument was checked in detail for bulk Pt where the density of states (DOS) of both methods are in perfect agreement.

In order to go further in the comparison between the two methods, we have analyzed the distribution of the charge between the *s*, *p*, and *d* orbitals in the muffin-tin sphere (MTS) of the FLAPW method and in the *s*, *p*, and *d* orbitals of the TB basis set. In Table I, we present the number of electrons in each orbital for the bulklike atom (C), the surface (S), and subsurface (S−1) atoms. Note that the MTS volume is about half the atomic volume. The comparison between the total populations per atom given by TB and in the MTS given by FLAPW shows that the *d* electrons are strongly localized in the MTS, as stated above, while the *s* and *p* electrons are almost equally shared in the MTS and in the remaining volume. Moreover, it is worthwhile to observe that on the surface atoms of the three surfaces there is a decrease of the total charge in the MTS, this change being mainly due to the decrease of the *p* population.

We have also calculated the work function (at 0 K) for each surface orientation with the FLAPW method using the film geometry. Unfortunately, the *spd* TB method does not

TABLE II. Work functions (in eV) of flat surfaces.

Orientation	FLAPW-LDA	Others	Expt.
(111)	6.53	6.07;[a] 6.74;[b] 6.12[c]	
(100)	6.52	6.97[b]	5.77–6.10[d]
(110)	6.19		

[a]See Ref. 33.
[b]See Ref. 13.
[c]See Ref. 61.
[d]See Refs. 62–65.

TABLE III. Surface energies $E_S(hkl)$ of low index surfaces of platinum calculated using the *spd* TB and FLAPW methods compared with previous results from Refs. 13, 16, and 37. The experimental value is also reported (Ref. 2). All results are given in eV/(surface atom) and refer to unrelaxed surfaces.

Orientation	FLAPW-LDA	FLAPW-GGA	*spd* TB	LMTO-GGA	KKR-LDA	LMTO-LDA	Experiments
(111)	1.10	0.85	1.01	1.00	0.96	0.98	1.03
(100)	1.50	1.16	1.45	1.38	1.27	1.19	
(110)	2.26	1.70	2.18	2.01	1.97		

allow us to have access to this physical quantity. Our results are listed in Table II together with other theoretical calculations and experiments. The work functions of the (111) and (100) faces are nearly the same while the values obtained by Skriver and Rosengaard[13] exhibit a deviation of 3%. It should be noted that in the case of Ag,[13] theoretically calculated work functions of the (111) and (100) faces were found to be nearly identical. At this stage, we cannot conclude whether this difference is realistic or not. The Pt work functions W obey the relation:

$$W_{(111)} > W_{(100)} > W_{(110)}. \qquad (10)$$

Note however, that the (110) surface exhibits a (1×2) reconstruction at equilibrium. These inequalities can be explained on the basis of geometric considerations. In general, one expects the work function to decrease as the surface becomes more open due to the smoothing of the modulation of the electron density at the surface. This argument apparently applies to Pt surfaces. Finally, compared to the work functions of Skriver and Rosengaard, our values are closer to experiment since it is known that the work function decreases slightly with temperature. It should also be mentioned that reconstruction could modify the work function value. In particular the (100) surface is metastable and can undergo several reconstructions, the (1×5) being the most common one.[35,36]

B. Surface energies of low-index surfaces

Let us now discuss the surface energies of the three main flat surfaces. In a first step, no atomic relaxation has been allowed. In the FLAPW approach, a 13-layer slab was used to model the (111) surface, 15 layers for the (100) orientation, and a 19-layer slab for the (110) surface. These slabs are repeated periodically and separated by 5, 5, and 8 vacuum layers for the (111), (100), and (110) surfaces, respectively. Within the *spd* TB method, 13-layer slabs were used for (111) and (100) surfaces and 17 layers for the (110) surface. In both cases it was checked that increasing the number of layers does not change the surface energy significantly. The surface energies per surface atom were then defined by

$$E_S(hkl) = \frac{1}{2}[E_{hkl}(n) - nE_{\mathrm{bulk}}], \qquad (11)$$

where $E_{hkl}(n)$ is the total energy per unit cell of the slab, and E_{bulk} is the bulk energy per atom and n is the number of atomic layers in the slab. Note that for the calculation of surface energies, the determination of the bulk energy is critical. This energy can be extracted from a true bulk calculation or from the difference of two slab calculations. We have checked that both procedures give the same results if the number of layers is large enough to achieve the energy convergence. The different results are listed in Table III. The values reported previously by Vitos *et al.*,[16] Galanakis *et al.*,[37] and Skriver and Rosengaard[13] are also reported for comparison. One first notes that the values for the surface energies obtained with GGA are the smallest ones reported in this table, even though Vitos *et al.* used also the GGA in their calculations. The FLAPW-LDA values and *spd* TB ones are quite similar and differ at most by 9%. These values are the largest and are closer to those calculated by Vitos *et al.* Discrepancies between the FLAPW-LDA method and other methods have been already reported by Galanakis *et al.*[38] in the case of Au surfaces. However, for Au the values obtained using the full-potential Korringa-Kohn-Rostoker (FKKR) method are larger than the FLAPW-LDA ones.

TABLE IV. Unrelaxed surface energy and work function of Pt(100) given by several LDA exchange correlation potentials at fixed lattice parameter (3.92 Å).

Exchange correlation potential	Surface energy (eV/atom)	Work functions (eV)
Moruzzi, Janak, and Williams[a]	1.50	6.21
von Barth and Hedin[b]	1.53	6.57
Vosko, Wilk, and Nusair[c]	1.50	5.96
Perdew and Zunger[d]	1.50	6.12

[a]Reference 66.
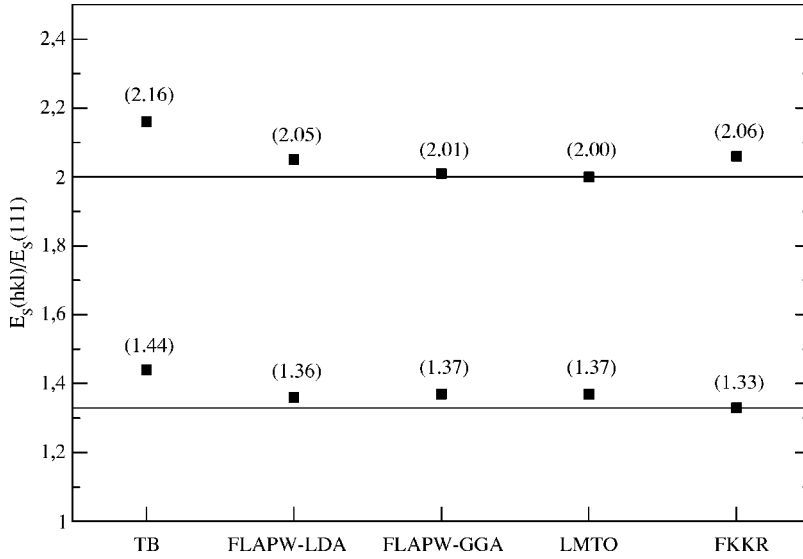[b]Reference 24.
[c]Reference 42.
[d]Reference 43.

FIG. 3. The anisotropy ratios of surface energies (per atom) for platinum, $E_S(100)/E_S(111)$ (lower values) and $E_S(110)/E_S(111)$ (upper values), using *spd* TB, FLAPW, LMTO from Ref. 16 and FKKR from Ref. 38 methods. The two solid lines represent the ideal first-neighbor broken-bond ratios: 4/3 for (100) and 2 for (110).

Actually, the surface energy may be sensitive to the technical details and approximations made in the calculation. Thus we have carried out several computations in order to check the accuracy of our results. First, we have verified the convergence with respect to the number $N_{k_\parallel}$ of $k_\parallel$ points. Indeed, in Ref. 38, the authors have shown that, at least for the (111) face, the surface energy is very sensitive to $N_{k_\parallel}$ (Fig. 2 of Ref. 38). We have recalculated the surface energy of the (111) face with $N_{k_\parallel}=300$ instead of 57 within the LDA. The value obtained [1.12 eV/(surface atom)] is similar to the one previously calculated [1.10 eV/(surface atom)], i.e., the convergence was achieved since these two energies differ only by 2%. This feature contrasts with the study of the noble metals done by Galanakis *et al.* in which the value of the surface energy was much more sensitive to $N_{k_\parallel}$. As explained in Ref. 37, unlike the (111) surface of fcc transition metals, noble metals exhibit an occupied surface state centered at the $\bar{\Gamma}$ point just above the d band, and thus a very dense $k_\parallel$-point grid is needed in the calculations of the slab total energy for the latter elements.

Second, still considering the (111) face, we have also tried to estimate the effect of spin-orbit (SO) coupling and also of relativistic corrections of MacDonald and Vosko[39] introduced in the XC potential in LDA. Indeed, these corrections may be important for the heavy elements of the $5d$ series. We have first recalculated the lattice parameter introducing the SO coupling. For LDA (3.91 Å), the agreement with the ex-

perimental value becomes as good as the one obtained with *spd* TB method while in GGA we get 4.01 Å. The relativistic corrections to the XC potential do not modify the values of the surface energy obtained previously. In contrast, the surface energy is more sensitive to the introduction of the SO coupling since it leads to an energy equal to 0.90 eV/(surface atom). This decrease of the surface energy can be understood qualitatively using a simple TB model limited to the d band. In this model the total energy is split into two contributions, a band term and a repulsive term,[8] the former being the leading one. In the usual approximation where only intra-atomic matrix elements of the spin-orbit coupling interaction are taken into account, the second moment of the LDOS of an atom in the (111) surface and in the bulk are respectively $9\beta^2+3\xi^2/2$ and $12\beta^2+3\xi^2/2$, where β is an effective hopping integral between nearest neighbors[40] and ξ the spin-orbit parameter. The ratio of the band contribution to the surface energy with and without spin-orbit coupling is given by[8]

$$\frac{E_S^{band}(\xi)}{E_S^{band}(0)} = \frac{\sqrt{12\beta^2+3\xi^2/2}-\sqrt{9\beta^2+3\xi^2/2}}{\sqrt{12\beta^2}-\sqrt{9\beta^2}}. \quad (12)$$

For Pt $\beta\simeq0.41$ eV (Ref. 40) and $\xi\simeq0.62$ eV (Ref. 41) we find $E_S^{band}(\xi)/E_S^{band}(0)=0.86$, to be compared with the value 0.82 found in FLAPW calculations.

Third, the choice of the XC potential could also be tested. A large variety of XC potentials in the LDA approximation

TABLE V. Relaxed surface energies and relaxation of the inter-planar distances Δd_{ij} (in %) for ideal low index surfaces of Pt calculated from FLAPW-LDA and *spd* TB.

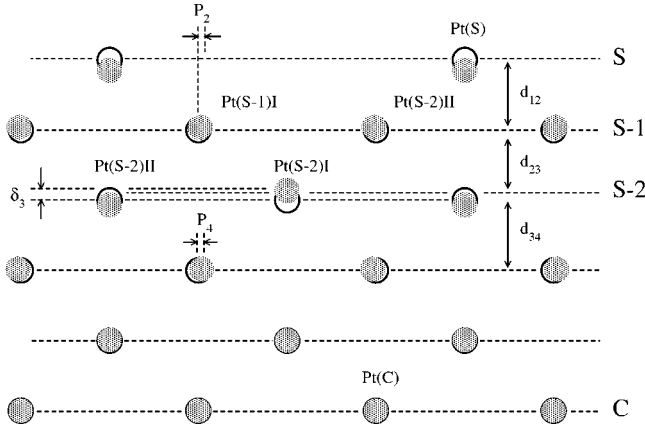|	Pt(111)			Pt(100)		Pt(110)	
	FLAPW	TB		FLAPW	TB	FLAPW	TB
Surface energy (eV/atom)	1.10	0.98	Experiments[a]	1.49	1.45	2.16	2.04
Δd_{12} (%)	+1.3	+3.8	+1.1	−1.9	−0.5	−14.0	−16.7
Δd_{23} (%)	+0.3	+0.2	+0.2	+0.3	+0.4	+8.3	+12.4
Δd_{34} (%)	+0.5	−0.4	-	+0.9	+0.04	−0.8	−3.0

[a]Reference 48.

FIG. 4. Schematic drawing of the geometry of the missing-row structure for the (1×2) Pt(110) surface. Shaded circles correspond to the relaxed positions and empty circles the unrelaxed ones.

can be found in the literature.[24,42,43] We have compared in Table IV the surface energy and the work functions of Pt(100) using a number of these potentials. Note that we have used the same lattice parameter, namely the experimental one (3.92 Å). The four XC potentials give almost the same surface energy, the largest difference being of the order of at most 2%. Note that the work functions depend more strongly on the choice of the XC potential, as was already mentioned by Alden *et al.*[44] for Ni(100).

Fourth, the cutoff (k_{max}) of the wave vector in the plane-wave expansion of the wave functions may be too small to describe the wave functions outside the MTS. For the (100) face, we have done a calculation with $k_{max}=4.8$ a.u. in order to check the validity of our first choice. With this new cutoff, the surface energy is also equal to 1.50 eV/atom. Thus increasing k_{max} does not modify the surface energy.

According to these checks, LDA seems to be a good compromise to get a realistic description of platinum surface energies. In addition, LDA gives better agreement with experiment for the atomic volume. Note, however, that, as already stated the bulk modulus is better described in GGA. These slight differences have been already largely discussed in the literature.[45,46] Nevertheless, it should be noted that the anisotropy ratios $E_S(hkl)/E_S(111)$ given by LDA and GGA (Fig. 3) are almost the same while *spd* TB gives slightly larger values. Galanakis *et al.*[37] have suggested that the transition-metal surfaces usually follow the broken-bond rule but with larger deviations than for noble metals because their *d* band is not filled and their LDOS present peaks at the Fermi level

depending on the surface orientation. The number of nearest-neighbor bonds broken by the surface is 3, 4, and 6 for the (111), (100), and (110) orientations, respectively. Actually LMTO, FKKR, and FLAPW give results very close to 4/3 for $E_S(100)/E_S(111)$ and to $6/3=2$ for $E_S(110)/E_S(111)$. In the following, we will only present results corresponding to LDA calculations and compare them with those obtained with the *spd* TB method.

The relaxation of the three flat surfaces has also been investigated. The relaxation of the interplanar distance between planes i and j is expressed as the ratio $\Delta d_{ij}=(d_{ij}-d_0)/d_0$ (in %), where d_{ij} is the interlayer spacing between the layers i and j, and d_0 is the interlayer spacing distance in the clean unrelaxed surface. Within the *spd* TB method, all layers were relaxed whereas in the case of the FLAPW method, only the three outermost layers were allowed to move. We have verified the validity of this assumption on the (100) face considering the relaxation of a larger number of planes. In Table V the structural parameters and the relaxed surface energies are presented. As expected, the surface energies of relaxed surfaces are slightly smaller (from −0.07% to −6.5%) with respect to the unrelaxed cases, the largest deviation being observed for the most open (110) surface. Indeed the (110) surface exhibits a large inward contraction of the first interlayer spacing by −14% (FLAPW) or −16.7% (*spd* TB), and an expansion of the second interlayer spacing by +8.3% (FLAPW) or +12.4% (*spd* TB). Note that the FLAPW results are very similar to those obtained by Jenkins *et al.*[47] using another *ab initio* code, and that the *spd* TB model has a tendency to overestimate the contractions or expansions of the distance between the layers. On the (111) face, both approaches agree in predicting an outward relaxation of the top layer (also verified by experiments[48]). Whereas it reaches a value of +3.8% with *spd* TB, it amounts to only +1.3% with the FLAPW, in very good agreement with the experimental results of Materer *et al.*[48] For the (100) face, contrary to the two former ones, the *spd* TB model seems to underestimate the first interlayer contraction compared to FLAPW but once more, the general tendencies are similar.

In the case of platinum, it is nowadays well known and observed experimentally, as well as found theoretically, that the (110) face exhibits a (1×2) missing-row reconstruction. The experimental studies reveal a considerable variation of the first interplanar distance: −0.26 Å or −0.28 Å by low-energy electron diffraction,[49,50] −0.42 Å by x-ray photoemission diffraction,[51] and −0.5±0.1 Å by neutral impact collision ion-scattering spectroscopy.[52] On the theoretical side, a

TABLE VI. The relaxed structural parameters for the reconstructed Pt(110)-(1×2) surface [P_i denotes pairing displacements in the *i*th row; δ_3 denotes buckling in the third Pt layer (see Fig. 4)].

Δd_{12} (%)	Δd_{23} (%)	Δd_{34} (%)	Δd_{45} (%)	P_2 (Å)	δ_3 (Å)	P_4 (Å)	References
−18.8	+0.5	+1.7	+1.4	0.04	0.28	0.07	Present results FLAPW
−26	−3.7	−1.5	+2	0.05	0.42	0.08	Present results *spd* TB
−16	0	+2	0	0.03	0.27	0.07	Theory (Ref. 47)
−17.6	−0.5	-	-	0.04	0.25	0.11	Theory (Ref. 57)
−20.8	−1.1	−1.1	+0.4	0.05	0.17	0.05	Experiments (Ref. 50)

TABLE VII. Surface energies and reconstruction energies in eV per (1×2) cell for the ideal (1×1) and reconstructed (1×2) (110) Pt surfaces.

	FLAPW	*spd* TB
(1×1) unrelaxed	4.36	4.36
(1×1) relaxed	4.17	4.10
(1×2) unrelaxed	4.23	4.16
(1×2) relaxed	3.93	3.63
Reconstruction energy (unrelaxed)	−0.13	−0.20
Reconstruction energy (relaxed)	−0.24	−0.47

Slater-Koster parametrized TB scheme[53,54] predicted rather smaller relaxations, whereas the EAM[55,56] and FLAPW[57] methods gave results comparable to most of the experimental values. We have also studied this reconstructed structure by means of our two approaches. In order to go further than Lee *et al.*,[57] who also used a full-potential technique but with slabs of seven layers only, we have modeled the (1×2) Pt(110) surface by a single slab consisting of eleven layers instead of seven. This choice was made in order to decrease finite size effects that are present in the Lee *et al.* calculations since their results show that the atoms belonging to the central layer have an atomic environment still significantly perturbed from the bulk one. On the surface layer on each side of the slab the missing-row structure was assumed and the slab was repeated periodically with 8 vacuum layers (Fig. 4). With the FLEUR code the Kohn-Sham equation was solved at 24 $\mathbf{k}_\parallel$ points within the irreducible wedge of the 2DBZ. The *spd* TB calculations were carried out for a 17-layer slab using 64 $\mathbf{k}_\parallel$ points. Our results for the structural parameters are presented in Table VI. The outermost interlayer spacing shows a significant contraction of $\Delta d_{12} = 18.6\%$ (FLAPW) and $\Delta d_{12} = 26\%$ (*spd* TB) with respect to the bulk distance. In addition, a large vertical buckling δ_3 in the third layer, and a lateral row pairing in the second (P_2) and fourth (P_4) layers are observed. They reproduce, especially within the FLAPW approach, the calculations of Lee *et al.*[57] and Jenkins *et al.*[47] and corroborate the experimental findings. Table VII gives the surface energy per (1×2) unit cell for the ideal and reconstructed Pt(110) in the relaxed and unrelaxed cases. The reconstruction energies, namely the surface energy difference between the (1×2) and (1×1) phases per (1×2) unit cell, are also reported. The two methods conclude to a stabilization of the system by the missing-row reconstruction. Relaxation reinforces this behavior. The surface energies obtained by the TB method tend to overestimate the reconstruction energies especially if one compares the re-
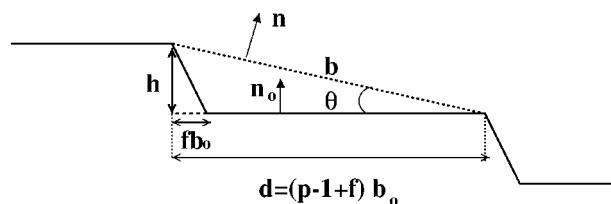

FIG. 5. Cut of a vicinal surface through a plane normal to the step edges: b is the distance between two consecutive steps, b_0 is the distance between two consecutive rows in a terrace, θ is the misorientation angle and p the number of atomic rows (including the inner edge) parallel to the step edge in a terrace, f is a geometrical factor depending on the vicinal surface, and h is the interplanar spacing along the direction normal to the terraces.

laxed value (−0.47 eV) to the value given by Jenkins *et al.*[47] (−0.2 eV). In contrast, the FLAPW value of the reconstruction energy is in better agreement with the one given by Jenkins *et al.* Finally, it should be noticed that the surface energies obtained with FLAPW for the ideal (1×1) surface per (1×2) unit cell are not exactly twice those given in Table III (unrelaxed case) and Table V (relaxed case). These slight discrepancies are due to the different number of layers included (11 instead of 17, respectively) and also, may be due the different $\mathbf{k}_\parallel$ point samplings in the (2×1) and the (1×1) cell.

C. From low-index surfaces to vicinal surfaces

We consider vicinal surfaces presenting a periodic succession of terraces with equal widths, separated by steps of monoatomic height (see Fig. 5). Using the simple model proposed by Vitos *et al.*,[58] we have calculated the energies of different kinds of isolated steps. Starting from the (111), (100), and (110) surface energies three effective pair potentials (EPP) V_s $(s = 1, 2, 3)$ can be evaluated using the following relation:

$$E_S(hkl) = \sum_{s=1}^{3} n_s(hkl) V_s. \tag{13}$$

In this expression, $n_s(hkl)$ is the number of broken bonds in the sth coordination shell for a surface of indices (hkl). Using the surface energies (see Table III) for each method the values of V_1, V_2, and V_3 have been determined and are listed in Table VIII. From these pair potentials, the energy of an isolated step can be expressed as:

TABLE VIII. The effective pair interactions in eV derived from the surface energies of Table III. The values obtained using the LMTO-GGA values of the surface energies can also be found in Ref. 58.

Pair interactions	FLAPW-LDA	*spd* TB	LMTO-GGA	KKR-LDA
V_1	0.410	0.441	0.316	0.38
V_2	−0.017	−0.055	−0.0197	0.002
V_3	−0.007	−0.012	0.0096	−0.016

TABLE IX. Calculated step energies for several vicinal surfaces of platinum using the effective pair potential model (EPP).

Stepped surface orientation	Miller indices	EPP	FLAPW-LDA	*spd* TB	LMTO-GGA	KKR-LDA
$p(111)\times(100)$	$(p+1,p-1,p-1)$	$2V_1+4V_3$	0.792	0.832	0.670	0.697
$p(111)\times(\bar{1}11)$	$(p-2,p,p)$	$2V_1+4V_3$	0.792	0.832	0.670	0.697
$p(100)\times(111)$	$(1,1,2p-1)$	V_1+2V_2	0.376	0.330	0.277	0.384
$p(100)\times(010)$	$(0,1,p-1)$	$2V_1+2V_2$	0.786	0.771	0.593	0.764
$p(110)\times(111)$	$(2p-1,2p-1,1)$	V_2+2V_3	−0.048	−0.080	−0.001	−0.029

$$E_{\text{step}}(p) = \sum_{s=1}^{3} n_{\text{step},s}(p)V_s,$$

$$n_{\text{step},s}(p) = n_s(p) - (p-1+f)n_s(\infty),$$

(14)

where p characterizes the number of atomic rows (including the inner edge) parallel to the step edge in a terrace, and f is a geometrical factor depending on the vicinal surface (see Fig. 5). The numbers $n_s(p)$ and $n_s(\infty)$ are the total number of bonds in the sth coordination sphere broken by the vicinal and flat surfaces, respectively. Due to the short range of the EPP, $n_{\text{step},s}(p)$ becomes a constant as soon as p overcomes a value p_∞, which is actually very small: most often, according to Vitos *et al.*,[58] $p_\infty \leq 2$. Raouafi *et al.*[59] have shown that the method proposed by Vitos *et al.* is quite valid if an estimation of step energies to $\approx 10^{-2}$ eV is needed and step-step interactions as well as atomic relaxation are disregarded. Using Eq. (14), we have calculated the step energies corresponding to stepped surfaces with either (111), (100), or (110) terraces. The results are listed in Table IX. The agreement between all results is reasonable for the stepped surfaces with (111) terraces. Considering the vicinal surfaces with (100) terraces, for which the value of V_2 plays an important role, larger differences are found. From Table V it is indeed seen that the value of V_2 is strongly dependent on the

surface energy database. For example, using the energy database of Galanakis *et al.*,[38] V_2 is positive, contrary to the other methods. In addition, all calculations give a very small negative step energy on the vicinal surfaces with (110) terraces for steps with (111) ledge orientation. This shows that the ideal (110) surface is not the most stable one as discussed in details in Refs. 58 and 60. Indeed, as stated above, the (110) surface of Pt exhibits a (1×2) missing-row reconstruction.

In order to conclude this study of the platinum surfaces and also to make comparisons between the two methods, we have carried out similar calculations for the unrelaxed $6(111)\times(\bar{1}11)$ [or (233)] vicinal surface. Figure 6 gives the geometry of this surface and indicates the geometrically inequivalent atoms in the unit cell when the vicinal system is modeled by slabs of 45 layers oriented in the [233] direction separated by 20 vacuum layers. In FLAPW calculations the convergence was achieved using 5 $\mathbf{k}_\parallel$ points in the irreducible wedge of the 2DBZ and the LDOS were computed with 40 $\mathbf{k}_\parallel$ points. With the TB method 64 $\mathbf{k}_\parallel$ points were used in the irreducible wedge. Within TB calculations, E_{step} is found to be equal to 0.815 eV and is very close to the value determined with the EPP approach. FLAPW calculations give a smaller value (0.582 eV). In Fig. 7, we present the LDOS of different atoms of the stepped surface. It is seen that the
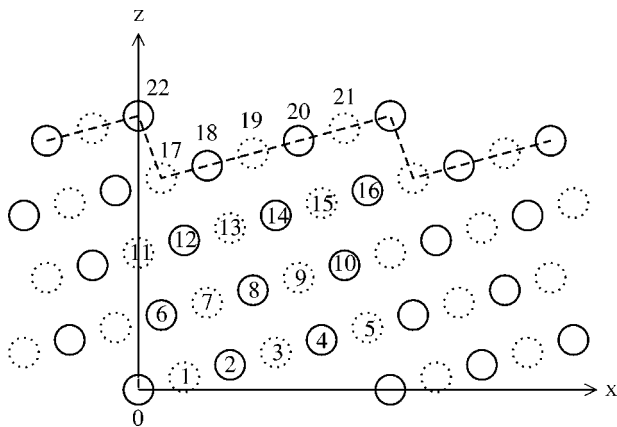

FIG. 6. Cross section by a plane perpendicular to the step edges of the $6(111)\times(\bar{1}11)$ or (233) Pt vicinal surface. Empty circles correspond to atoms in the plane $y=0$ whereas dotted circles correspond to atoms in the plane $y=a/2$, a being the nearest-neighbor distance. The geometrically inequivalent atoms in the unit cell of the 45-layer slab used in the calculations are labeled from 0 to 22.
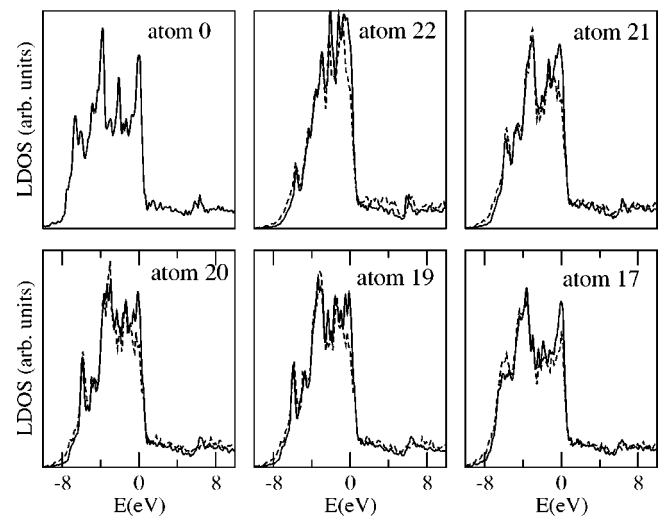

FIG. 7. The local densities of states obtained from FLAPW (full lines) and *spd* TB (dashed lines) for different atoms of the Pt(233) vicinal surface. The numbering of atoms is defined in Fig. 6. The origin of the energy scale refers to the Fermi energy.

agreement between TB and FLAPW LDOS is quite good. From the LDOS, we can say that contrary to rhodium for which outer step edges might become magnetic depending on the step geometry,[59] it is unlikely that platinum becomes magnetic at least for this step configuration. Indeed the LDOS at the Fermi level are not enhanced compared to the bulk one even on the outer edge atom. Thus, according to the Stoner model, no local magnetic moment is expected.

IV. CONCLUSION

In this paper we have made a careful investigation of the electronic structure of platinum surfaces by comparing two different approaches. We have used a nonorthogonal basis set of s, p, and d valence orbitals in the tight-binding scheme in order to better describe the cohesive properties of platinum. The sources of uncertainties inherent to DFT calculations have been carefully analyzed in the FLAPW method implemented in the FLEUR code. In particular, LDA and GGA approximations have been investigated. Different exchange-correlation potentials were tested. Thick slabs were considered in order to definitely rule out finite size effects. In addition, parameters such as the number of $\mathbf{k}_\parallel$ points, the cutoff $k_{\max}$ for the plane-wave expansion, and relativistic ef-

fects were also checked. We show that the surface energy of the (111) surface and the relaxation of the three low-index surfaces agree well with the experimental findings using TB as well as FLAPW-LDA methods. An outward relaxation is found for Pt(111) while less close-packed surfaces [(100) and (110)] exhibit inward relaxations. However, it is well known that the (110) surface undergoes a (1×2) missing-row reconstruction and, indeed, the calculated surface energy of this structure is smaller than that of the ideal (110) surface. Following the effective pair potential method developed by Vitos *et al.*, we have calculated the step energies for various step geometries. Finally, we have carried out full calculations on the (233) vicinal surface and found that the LDOS were nearly identical with the LDA and TB methods. In the near future, we would like to extend this study by considering metallic adsorbed species (growth, equilibrium structures, and electronic properties) on flat and stepped Pt substrates.

ACKNOWLEDGMENTS

*Author to whom correspondence should be addressd. Email address: stephanie.baud@univ-fcomte.fr

[1] V. K. Kumikov and Kh. B. Khokonov, J. Appl. Phys. **54**, 1346 (1983).

[2] W. R. Tyson and W. A. Miller, Surf. Sci. **62**, 267 (1977).

[3] F. R. Boer, R. Boom, W. C. M. Mattens, A. R. Miedema, and A. K. Niessen, *Cohesion in Metals* (North-Holland, Amsterdam, 1988).

[4] M. S. Daw and M. I. Baskes, Phys. Rev. B **29**, 6443 (1984); Z.-J. Tian and T. S. Rahman, *ibid.* **47**, 9751 (1993).

[5] F. Ducastelle, J. Phys. (Paris) **31**, 1055 (1970).

[6] K. W. Jacobsen, J. K. Norskov, and M. Puska, Phys. Rev. B **35**, 7423 (1987); K. W. Jacobsen, P. Stoltze, and J. K. Norskov, Surf. Sci. **366**, 394 (1996).

[7] A. P. Sutton and J. Chen, Philos. Mag. Lett. **61**, 139 (1984); M. W. Finnis and J. M. Sinclair, Philos. Mag. A **50**, 45 (1984).

[8] M. C. Desjonquères and D. Spanjaard, *Concepts in Surface Physics* (Springer, New York, 1995), and references therein.

[9] M. C. Desjonquères and F. Cyrot-Lackmann, Surf. Sci. **50**, 257 (1975).

[10] S. Papadia, M. C. Desjonquères, and D. Spanjaard, Phys. Rev. B **53**, 4083 (1996).

[11] M. J. Mehl and D. A. Papaconstantopoulos, Phys. Rev. B **54**, 4519 (1996). The parameters are available in a computationally accessible form at http://cst-www.nrl.navy.mil/bind/index.html

[12] M. Methfessel, D. Hennig, and M. Scheffler, Phys. Rev. B **46**, 4816 (1992).

[13] H. L. Skriver and N. M. Rosengaard, Phys. Rev. B **46**, 7157 (1992).

[14] M. Alden, H. L. Skriver, S. Mirbt, and B. Johansson, Phys. Rev. Lett. **69**, 2296 (1992).

[15] P. J. Feibelman, Phys. Rev. B **52**, 16 845 (1995).

[16] L. Vitos, A. V. Ruban, H. L. Skriver, and J. Kollàr, Surf. Sci. **411**, 186 (1998), and references therein.

[17] H. J. F. Jansen and A. J. Freeman, Phys. Rev. B **30**, 561 (1984).

[18] C. L. Fu, S. Ohnishi, H. J. F. Jansen, and A. J. Freeman, Phys. Rev. B **31**, 1168 (1985).

[19] P. Gambardella, M. Blanc, H. Brune, K. Kuhnke, and K. Kern, Phys. Rev. B **61**, 2254 (2000), P. Gambardella, M. Blanc, K. Kuhnke, K. Kern, F. Picaud, C. Ramseyer, C. Girardet, C. Barreteau, D. Spanjaard, and M. C. Desjonquères, *ibid.* **64**, 045404 (2001).

[20] F. Picaud, C. Ramseyer, C. Girardet, and P. Jensen, Phys. Rev. B **61**, 16 154 (2000).

[21] $p(hkl) \times (h'k'l')$ indicates the type of vicinal surface using the notation introduced by Lang et al. [B. Lang, R. W. Joyner, and G. A. Somorjai, Surf. Sci. **30**, 440 (1972)]. (hkl) and $(h'k'l')$ denote, respectively, the orientations of the terraces and of the edges, and p is the number of atomic rows parallel to the edges (including the inner edge) on a terrace.

[22] E. Wimmer, H. Krakauer, M. Weinert, and A. J. Freeman, Phys. Rev. B **24**, 864 (1981); M. Weinert, E. Wimmer, and A. J. Freeman, *ibid.* **26**, 4571 (1982).

[23] This code can be found at the following web site: http://www.flapw.de

[24] U. von Barth and L. Hedin, J. Phys. C **5**, 1629 (1972).

[25] J. P. Perdew, J. A. Chevary, S. H. Vosko, K. A. Jackson, M. R. Pederson, D. J. Singh, and C. Fiolhais, Phys. Rev. B **46**, 6671 (1992).

[26] H. J. Monkhorst and J. D. Pack, Phys. Rev. B **13**, 5188 (1976).

[27] P. O. Löwdin, J. Chem. Phys. **18**, 365 (1950).

[28] N. Bernstein, M. J. Mehl, and D. A. Papaconstantopoulos, Phys.

Rev. B **66**, 075212 (2002).

[29] S. L. Cunningham, Phys. Rev. B **10**, 4988 (1974).

[30] N. W. Ashcroft and N. D. Mermin, *Solid State Physics* (Saunders College Publishing, Philadelphia, 1976).

[31] B. Ozoliņŝ and M. Körling, Phys. Rev. B **48**, 18 304 (1993).

[32] A. Khein, D. J. Singh, and C. J. Umrigar, Phys. Rev. B **51**, 4105 (1995).

[33] G. Boisvert, L. J. Lewis, and M. Scheffler, Phys. Rev. B **57**, 1881 (1997).

[34] J. L. F. Da Silva, Ph.D. Thesis, Technical University Berlin, Berlin, Germany, 2002 (http://edocs.tu-berlin.de/diss/2002/dasilva_juarez. htm).

[35] S. Hagstrom, H. B. Lyon, and G. A. Somorjai, Phys. Rev. Lett. **15**, 491 (1965).

[36] P. R. Norton, J. A. Davies, D. P. Jackson, and N. Matsunami, Surf. Sci. **269**, 85 (1979).

[37] I. Galanakis, N. Papanikolaou, and P. H. Dederichs, Surf. Sci. **511**, 1 (2002).

[38] I. Galanakis, G. Bihlmayer, V. Bellini, N. Papanikolaou, R. Zeller, S. Blügel, and P. H. Dederichs, Europhys. Lett. **58**, 751 (2002).

[39] A. K. MacDonald and S. H. Vosko, J. Phys. C **12**, 2977 (1979).

[40] Actually $\beta^2 = (dd\sigma^2 + 2dd\pi^2 + 2dd\delta^2)/5$. The values of $dd\sigma$, $dd\pi$, $dd\delta$ are taken from N. V. Smith and L. F. Mattheiss, Phys. Rev. B **9**, 1341 (1974).

[41] F. Herman and S. Skillman, *Atomic Structure Calculations* (Prentice-Hall, Englewood Cliffs, New Jersey, 1963).

[42] S. H. Vosko, L. Wilk, and M. Nusair, Can. J. Phys. **58**, 1200 (1980).

[43] J. P. Perdew and A. Zunger, Phys. Rev. B **23**, 5048 (1981).

[44] M. Alden, S. Mirbt, H. L. Skriver, N. M. Rosengaard, and B. Johansson, Phys. Rev. B **46**, 6303 (1992).

[45] S. Kurth, J. P. Perdew, and P. Blaha, Int. J. Quantum Chem. **75**, 889 (1999).

[46] M. Mansfield and R. J. Needs, Phys. Rev. B **43**, 8829 (1991).

[47] S. J. Jenkins, M. A. Peterson, and D. A. King, Surf. Sci. **494**, 159 (2001).

[48] N. Materer, U. Starke, A. Barbieri, R. Döll, K. Heinz, M. A. Van Hove, and G. A. Somorjai, Surf. Sci. **325**, 207 (1995).

[49] E. C. Sowa, M. A. Van Hove, and D. L. Adams, Surf. Sci. **199**, 174 (1988).

[50] P. Fery, W. Moritz, and D. Wolf, Phys. Rev. B **38**, 7275 (1988).

[51] S. Homlberg, H. C. Poon, Y. Jugnet, G. Grenet, and T. M. Duc, Surf. Sci. Lett. **254**, L475 (1991).

[52] S. Speller, S. Parascandola, and W. Heiland, Surf. Sci. **383**, 131 (1997).

[53] D. Tomanek, H.-J. Brocksch, and K. H. Bennemann, Surf. Sci. **138**, L129 (1984).

[54] H.-J. Brocksch and K. H. Bennemann, Surf. Sci. **161**, 321 (1985).

[55] S. M. Foiles, Surf. Sci. **191**, L779 (1987).

[56] M. S. Daw, Surf. Sci. **166**, L161 (1986).

[57] J. I. Lee, W. Mannstadt, and A. J. Freeman, Phys. Rev. B **59**, 1673 (1999).

[58] L. Vitos, H. L. Skriver, and J. Kollár, Surf. Sci. **425**, 212 (1999).

[59] F. Raouafi, C. Barreteau, M. C. Desjonquères, and D. Spanjaard, Surf. Sci. **505**, 183 (2002).

[60] L. Vitos, B. Johansson, H. L. Skriver, and J. Kollàr, Comput. Mater. Sci. **17**, 156 (2000).

[61] P. J. Feibelman, Phys. Rev. B **56**, 2175 (1997).

[62] M. Salmerón, S. Ferrer, M. Jazzar, and G. A. Somorjai, Phys. Rev. B **28**, 6758 (1983).

[63] G. N. Derry and J.-Z. Zhang, Phys. Rev. B **39**, 1940 (1989).

[64] A. Cassuto, M. Mane, M. Hugenschmidt, P. Dolle, and J. Jupille, Surf. Sci. **237**, 63 (1990).

[65] M. Kaack and D. Fick, Surf. Sci. **342**, 111 (1995).

[66] V. L. Moruzzi, J. F. Janak, and A. R. Williams, Phys. Rev. B **12**, 1257 (1975).